



Supplement of

Simulating dust emissions and secondary organic aerosol formation over northern Africa during the mid-Holocene Green Sahara period

Putian Zhou et al.

Correspondence to: Putian Zhou (putian.zhou@helsinki.fi) and Risto Makkonen (risto.makkonen@fmi.fi)

The copyright of individual parts of the supplement might differ from the article licence.

5

10 **Supplement**

15

1 LPJ-GUESS output data

The LPJ-GUESS output data used in this study were originally saved at each land grid out of the reduced Gaussian grid over the globe during the simulation years 1850 to 1859. Here the exact years do not mean anything but just represent the last 10 years of the simulation experiments, including the PI, MH and MH_gsrld cases (Lu et al., 2018). The raw data were from the simulations conducted in Lu et al. (2018), which include grid latitude and longitude, monthly low and high vegetation cover, dominant low and high vegetation type, and emissions of isoprene and monoterpenes.

The raw data are saved at Puhti which is a supercomputer in CSC. The columns in the vegetation cover files are longitude, latitude, year, 12-month LAI of low vegetation, 12-month LAI of high vegetation, 12-month of low vegetation cover, 12-month of high vegetation cover, dominant low vegetation type and dominant high vegetation type. The LAI unit is (leaf m²) (ground m⁻²). The rows are for all the land grids and all the years. The columns in the BVOC emission files are longitude, latitude, year, 12-month of monthly mean emissions in the unit of mg m⁻² mon⁻¹. The rows are the same as that in the vegetation files.

First all the raw vegetation data are interpolated to 1×1 grid the same as standard TM5 input meteorological data, and the raw BVOC emission data are interpolated to 0.5×0.5 grid the same as standard TM5-MP input MEGAN emission data. Here linear interpolation is applied for all variables except vegetation type which used nearest interpolation method. In TM5-MP

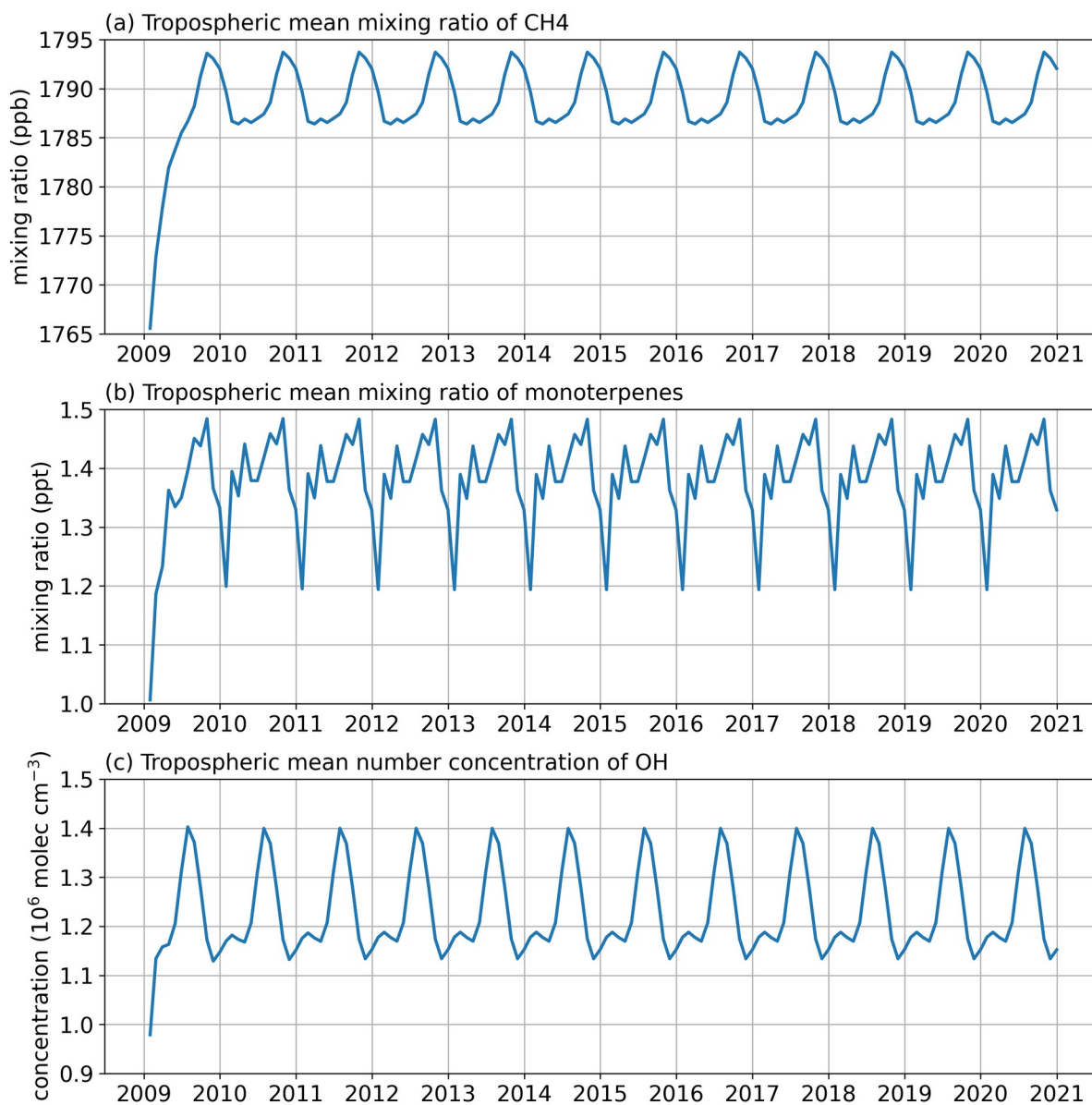
within one grid there are only one low and one high vegetation types, so the vegetation percentage of a specific type is either 100% or 0%.

35 **2 Generate TM5-MP input files from LPJ-GUESS output data**

The new TM5-MP input vegetation files for pi_ctrl, pi_zero, mh and mh_gsrd cases are generated according to the LPJ-GUESS output vegetation data, and the generated files only include monthly data instead of 6 hourly data in the default TM5-MP input vegetation files. The new TM5-MP input monthly BVOC emission data files are generated in the same way. Here the 10-year interannual average values of cvl (low vegetation cover), cvh (high vegetation cover) and BVOC emissions
40 for each month are used in the generated input files. While the tv (vegetation type) values are from the last simulation year (namely 1859) since we assume that the last-standing vegetation type is the dominant one.

3 BVOC emissions during the pre-industrial (PI) period

In order to compare our modelled BVOC emissions during the PI period to other studies, we obtained the 30-year simulated emission data from a recent study by Weber et al. (2022a, b) (labelled as Weber2022 below), in which the iBVOC emissions
45 system was applied to calculate the emissions of isoprene and monoterpenes during the PI (for more details refer to Weber et al., 2022a). Fig. S2 shows the comparison results over Africa between the cases pi_ctrl, pi_orig and Weber2022. The BVOC emissions data in pi_orig were taken from the MEGAN-MACC datasets for the year 2009, so it actually represents a present-day condition. The cases pi_orig and Weber2022 show similar emission patterns for both isoprene and monoterpenes emissions. The essential difference is that pi_orig shows larger latitudinal gradient than Weber2022. In pi_ctrl, the isoprene emis-
50 sion is more homogeneous in Central and Southern Africa compared to the other two cases, both of which show an apparent higher emission over Central Africa. For monoterpenes, pi_ctrl shows higher emissions in Southern Africa and lower emissions in Central Africa, while the other two cases present an opposite pattern. We should note that over Northern Africa, which is the domain of focus of this study, all of these PI cases show low to none emissions of isoprene and monoterpenes. It indicates that our main results and conclusions are not affected by the uncertainties of PI BVOC simulations.



FigureS 1: Time series of (a) tropospheric mean mixing ratio of methane (CH₄), (b) tropospheric mean mixing ratio of monoterpenes and (c) tropospheric mean number concentration of hydroxyl radical (OH) in a 12-year simulation. The input data of 2009 were applied repeatedly for each year, but the tick labels show increasing year numbers to represent the continuous simulation years. Here the tropospheric mean values are calculated over the first 21 model layers, in which the global mean air pressure of the top layer (layer 21) is around 200 hPa.

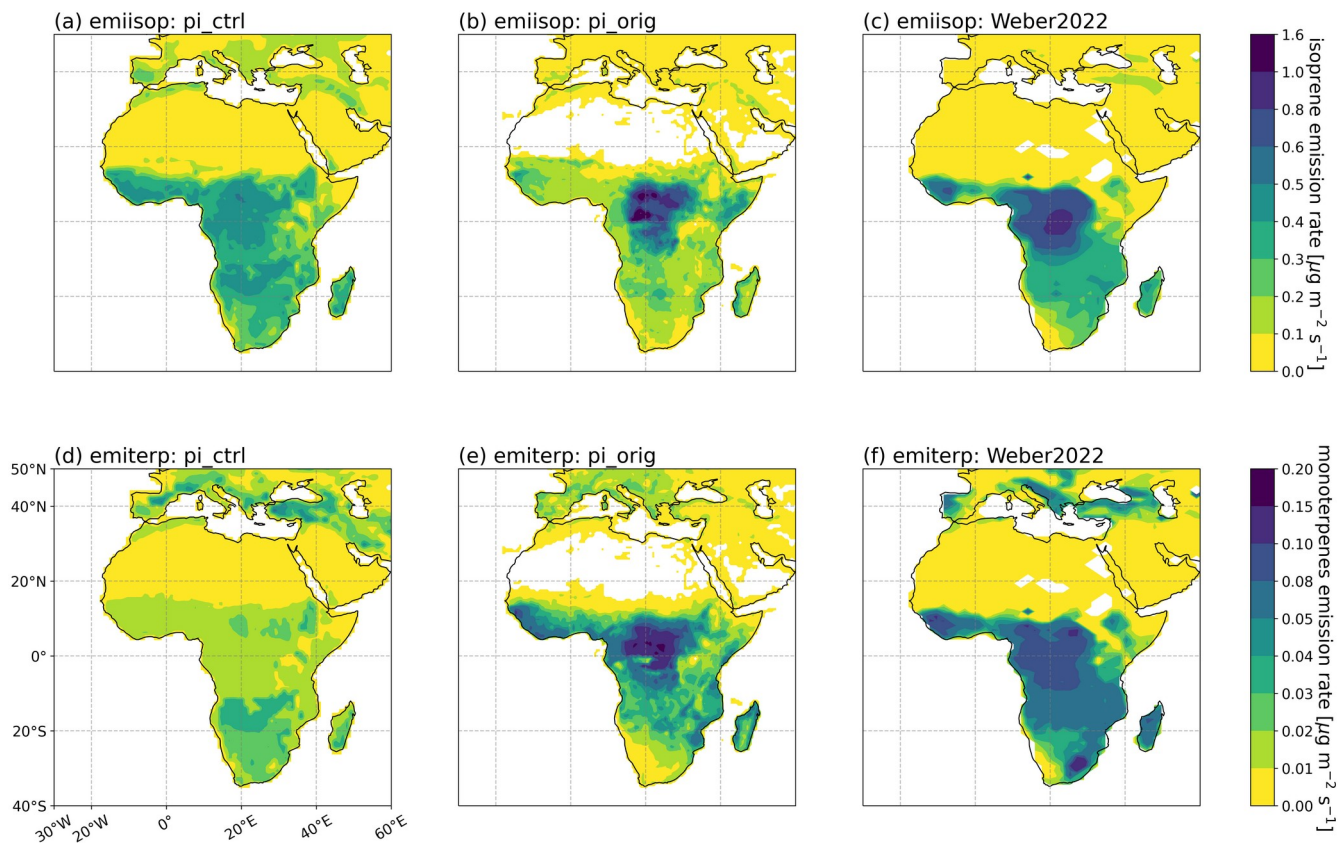
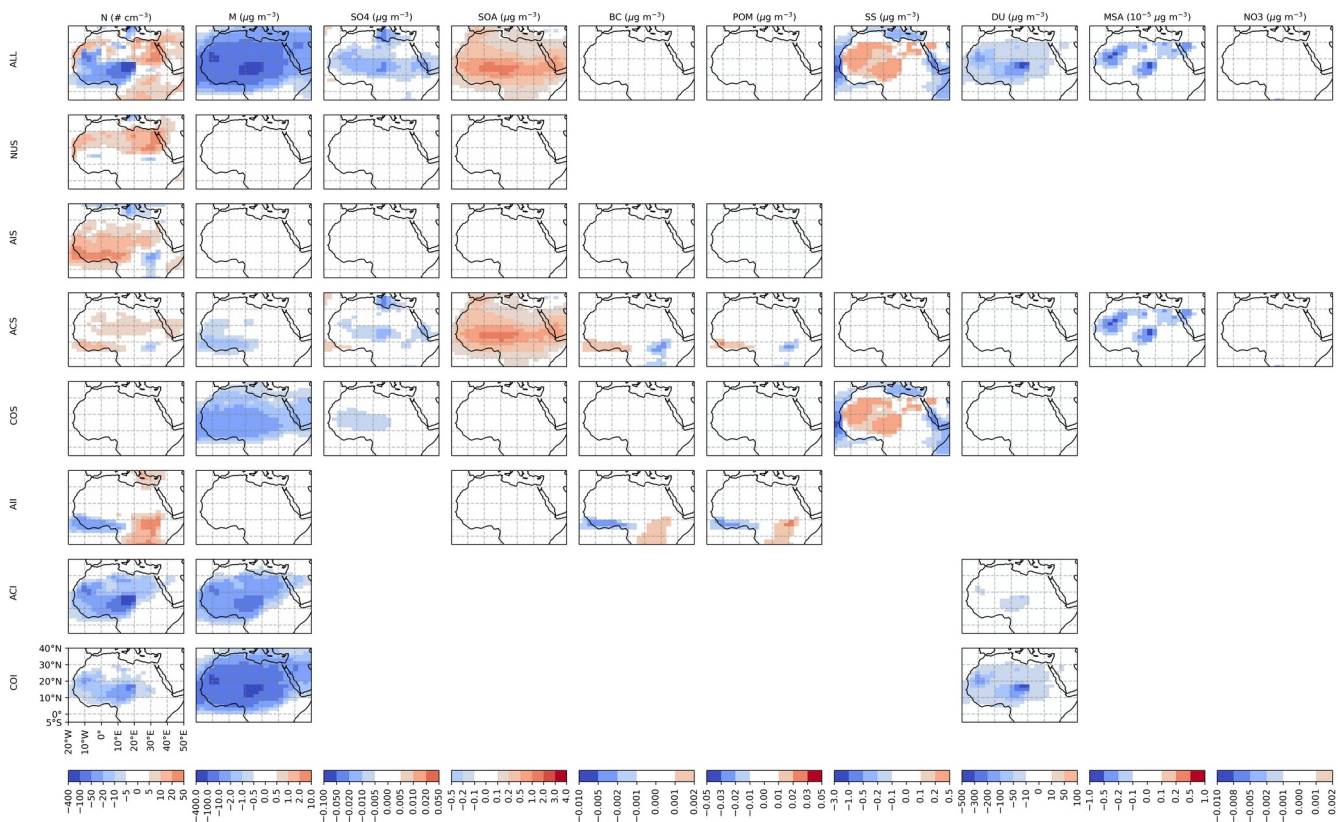


Figure S 2: Annual mean emission rates of isoprene (emiisop) over Africa from the simulation cases (a) pi_ctrl, (b) pi_orig and (c) the emission data from Weber et al. (2022a, b) (Weber2022). The annual mean emission rates of monoterpenes (emiterp) are also shown for simulation cases (d) pi_ctrl, (e) pi_orig and (f) Weber2022.



FigureS 3: The difference of various quantities between *mh* and *pi_zero*. The quantities in the first row include the total particle number concentration (*N*) in the unit of $\# \text{ cm}^{-3}$, the total particle mass concentration (*M*) in the unit of $\mu\text{g m}^{-3}$, the total mass concentrations of individual components in the particles including sulfate (*SO4*), *SOA*, black carbon (*BC*), primary organic matter (*POM*), sea salt (*SS*), dust (*DU*), methane sulfonic acid (*MSA*) and nitrate (*NO3*) in the unit of $\mu\text{g m}^{-3}$. The quantities in the rows two to eight are the same but for the particles in the soluble nucleation mode (*NUS*), soluble Aitken mode (*AIS*), soluble accumulation mode (*ACS*), soluble coarse mode (*COS*), insoluble Aitken mode (*AII*), insoluble accumulation mode (*ACI*), soluble coarse mode (*COI*), respectively. The components not included in a mode are not plotted. Notice that the values of *MSA* need to be multiplied by 10^{-5} .

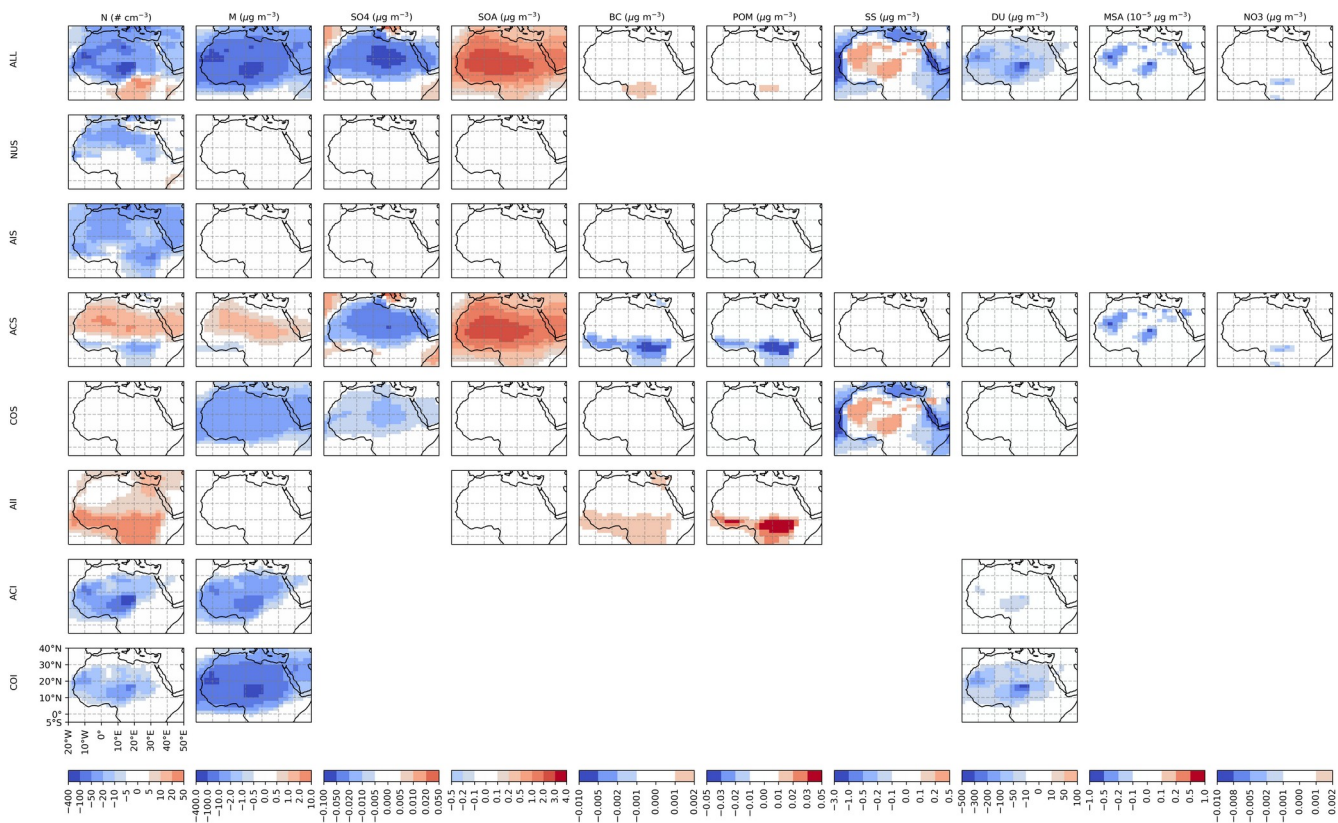


Figure S 4: The same as Figure S3 but showing the difference between *mh_gsr* and *pi_zero*.

60 **References**

Lu, Z., Miller, P. A., Zhang, Q., Zhang, Q., Wårlind, D., Nieradzik, L., Sjolte, J., and Smith, B.: Dynamic vegetation simulations of the mid-holocene green sahara. *Geophysical Research Letters*, 45(16):8294–8303, 2018.

Weber, J., Archer-Nicholls, S., Abraham, N. L., Shin, Y. M., Griffiths, P., Grosvenor, D. P., Scott, C. E., and Archibald, A. T.: Chemistry-driven changes strongly influence climate forcing from vegetation emissions. *Nat. Commun.*, 13, 7202, 2022a.

Weber, J., Archer-Nicholls, S., Abraham, N. L., Shin, Y. M., Griffiths, P., Grosvenor, D. P., Scott, C. E., and Archibald, A. T.: Research data supporting "Chemistry-driven oxidant changes strongly influence climate forcing from vegetation emission". Apollo - University of Cambridge Repository. <https://doi.org/10.17863/CAM.83526>. 2022b.